

Phase Separation of Aqueous Poly(vinyl methyl ether) Solutions Induced by the Photon Pressure of a Focused Near-Infrared Laser Beam

Yasuyuki Tsuboi,*[1,2] Masayuki Nishino,[1] Yasutaka Matsuo,[3] Kuniharu Ijiro,[3] and Noboru Kitamura*[1]

[1]Division of Chemistry, Graduate School of Science, Hokkaido University, Sapporo 060-0810

[2]SORST (Solution Oriented Research of Science and Technology), JST

[3]Research Institute for Electronic Science, Hokkaido University, Sapporo 060-0021

Received March 9, 2007; E-mail: twoboys@sci.hokudai.ac.jp

We demonstrate that phase separation of an aqueous poly(vinyl methyl ether) (PVME) solution can be triggered not only by a temperature change but also by photon pressure. A near-infrared continuous wave laser beam (λ = 1064 nm) was focused through an objective lens into a heavy water (D_2O) solution of PVME. A single PVME microparticle was produced and trapped at the focal point of the laser beam within several hundreds of seconds after switching on the laser. The origin of the microparticle formation (phase separation) is ascribed essentially to the photon force of the laser beam, and not to a rise in the local temperature, since heavy water is transparent at 1064 nm. The structures of the PVME microparticles produced by laser irradiation were studied in detail using confocal Raman microspectroscopy. Raman spectra of the microparticles and coiled/globular PVME were observed successfully over a wide wavenumber region. It was confirmed that the phase transition of the polymer chains from coiled to globular states proceeded during microparticle formation. The fundamental mechanism of photo-induced phase separation of PVME is discussed in terms of the interactions between the polymer and the photon force.

Interest in the chemistry of thermo-responsive artificial polymers, such as poly(*N*-isopropylacrylamide) (PNIPA), poly(vinyl methyl ether) (PVME), and their related derivatives, has undergone phenomenal growth over the past three decades, since the discovery of the thermal reversible phase separation of aqueous PNIPA solutions.[1,2] PNIPA homogeneously dissolved in water takes on a coiled structure at room temperature. Upon increasing the temperature ($\Delta T > 10$ K), the PNIPA coils turn into globules accompanied by dehydration of the polymer chains (phase transition), and subsequently, the solution undergoes phase separation due to aggregation of the globules by hydrophobic interactions.[3,4] Aqueous PVME solutions also show a thermo-responsive behavior analogous to that of PNIPA.[5] Relevant to the thermo-responsive phase transition and phase separation of these polymer solutions, polymer gels represented by cross-linked PNIPA and its derivatives are also known to exhibit intriguing thermo-responsive behavior.[6] Hydrated PNIPA gels shrink above a critical temperature ($\approx$310 K) accompanied by release of water (dehydration) from the gel. It has been reported that the characteristics and critical temperature of such phase transitions and phase separations depend upon several factors, such as the pH of the solution, the presence or absence of a chemical impurity (metal ions), and external physical perturbations (electric field, etc.), since the energetic balance regarding phase transition and separation is quite sensitive to these factors.[7,8]

The thermo-responsive behavior of these polymers or polymer solutions is quite intriguing from the viewpoint of the basic physicochemical polymer science. In addition, this family of polymers has promising potential in their application towards functional materials for water storage, drug delivery, selective material extraction, and so on.[7,8] Therefore, these intriguing processes of the thermo-responsive phase transition and separation of a polymer solution or gel coupled with hydration and dehydration of the polymer chains have been investigated in detail both experimentally and theoretically.

On the other hand, Masuhara and co-workers have recently found analogous phenomena with the thermo-responsive phase transition/separation of an aqueous PNIPA solution by means of a combination of an optical microscope and a near-infrared (NIR) laser beam.[9,10] A continuous wave (CW) 1064 nm laser beam is used to irradiate an aqueous PNIPA solution through an objective lens, causing the formation of PNIPA microparticle at the focal point of the laser beam. Since water (H_2O) absorbs light at the laser wavelength (1064 nm) through the overtone band of the O–H vibrational transition, the microparticle formation has been ascribed to local heating of the solution by laser irradiation. Importantly, despite the fact that heavy water (D_2O) is transparent at 1064 nm, analogous PNIPA microparticle formation to that in H_2O is observed even in D_2O.[11] In this case, local heating effects by laser irradiation are completely negligible. Therefore, the origin of microparticle formation is not due to photothermal effects, but due essentially to a pure electromagnetic force, called the photon pressure, which is described in the following paragraph.

When a laser beam is focused into a medium, a photon pressure is exerted on a microscopic particle in the focal region. The origin of the photon pressure is the dipole gradient force, and the force vector is directed to the center of a Gaussian laser beam when the refractive index (n) of the material is higher

Published on the web October 12, 2007; doi:10.1246/bcsj.80.1926

than that of the surrounding medium.[12] The photon force has been applied to laser manipulation techniques since the first demonstration by Ashkin.[13,14] In the laser manipulation technique, single microparticles in solution, such as living cells and polymer beads, can be trapped at the focal point of a laser beam.[15–20] Moreover, the photon pressure induces some intriguing phenomena in polymer systems.[21,22]

Laser-induced PNIPA microparticle formation in D_2O is due to the assembly of coiled PNIPA nanoparticles by photon force, since n of PNIPA is higher than that of water. The dimensions of these nanoparticles are of the order of several tens of nanometers. Furthermore, Juodkazis and co-workers have shown that the volume phase transition of a micro-rod-shaped PNIPA gel can be triggered by photon pressure exerted locally on the gel rod.[22] Thus, the laser-induced phenomena of PNIPA and related derivatives are novel and of great interest. However, little is known about the chemical structure of the material under photon pressure effects. Masuhara and co-workers have investigated the structures of PNIPA microparticles by using a fluorescence probe and have reported that the environment inside microparticles is hydrophobic.[23] To shed further light on the issue, more direct experimental approaches are needed to reveal the chemical structures under photon-pressure effects.

We consider Raman/IR spectroscopy to be one possible experimental tool for studying these phenomena. Indeed, Maeda and co-workers have examined polymer structures by systematically analyzing the changes in the vibrational spectra of PNIPA[24–27] and PVME[28–31] solution systems after thermo-responsive phase transition. Katsumoto et al. have also investigated the vibrational spectra of polymers both experimentally and theoretically.[32,33] Recently, we have developed a confocal Raman microscope combined with a laser trapping technique to gain access to the structure of a laser-induced microparticle.[34,35] The system has been applied to an aqueous PNIPA solution, and we have shown that the phase transition from the coiled to the globular state of PNIPA participates in microparticle formation.[34] In the present study, we applied the technique to PVME as another representative thermo-responsive polymer. Similarly to PNIPA, PVME has both hydrophilic (ether oxygen) and hydrophobic (polymer backbone and methyl side chain) groups. On the other hand, the molecular weight, refractive index, and the extent of the hydrophobic interactions between the polymer chains are somewhat different for PNIPA and PVME. On the basis of the experimental data on PVME and PNIPA, we demonstrated that phase transition followed by phase separation was induced by photon pressure.

Experimental

Sample Preparation. The samples examined in the present study were aqueous (H_2O and D_2O) PVME (4.0 wt %) solutions. PVME (Scientific Polymer Products, $M_w \approx 90000$, phase separation temperature: 308 K) was purified by successive re-precipitation of a toluene solution into *n*-heptane. (Wako, HPLC grade). The hydrodynamic radius of the polymer in water was evaluated to be 45 nm by dynamic light-scattering measurements (Otsuka Electronics, FDLS-3000). Since PVME is a well known hygroscopic polymer, special care was taken in preparing the heavy water samples in order to avoid contamination with H_2O from the air. PVME was dissolved in D_2O (Wako, 99.99% or Aldrich, 99.999%), stirred for several hours, and dried by evaporation of the solvent (heavy water) in vacuum. The solid PVME sample was dissolved again in heavy water. These procedures were repeated to completely substitute the H_2O with D_2O in the sample. Fresh samples were always used for the Raman spectroscopy employing a thin optical cell: the sample solution was placed between two glass plates, as reported previously.[34]

Confocal Raman Microspectroscopy. The experimental methods and apparatus have been reported elsewhere.[34,35] Briefly, a CW Nd^{3+}:YAG laser ($\lambda = 1064$ nm, Spectron Laser System, SL-902T) and a CW Ar^+ laser ($\lambda = 488$ nm, Coherent, Inova 70) were used for generating the photon pressure and excitation of the Raman scattering of the sample, respectively. The laser beams were introduced coaxially into an inverted optical microscope (Nikon, ECRIPSE E300) and irradiated on to the sample solution through an oil-immersion objective lens ($\times 100$, NA = 1.30). The 1064 laser beams was focused into a diffraction-limited spot of size d; $d = 1.22\lambda/\mathrm{NA} \approx 1\,\mu$m. Raman scattered light passed through a pinhole (100 μm) and two holographic notch filters (for 488 and 1064 nm) before being detected by a cooled CCD camera (Andor Tec.) equipped with a polychromator. The spatial resolutions in the lateral and vertical directions were 0.25 and 2.4 μm, respectively, and the spectral resolution was 2.0 cm^{-1}. The effective laser power (P_{eff}; laser power after passing through the objective lens) was measured using a power meter (Ophir, NOVA).[34] P_{eff} of the Ar^+ laser was kept at <5 mW that gave no any affection to the samples except for Raman effect. All the measurements were carried out at room temperature (21 °C), if not otherwise specified.

Results and Discussion

Laser-Induced Microparticle Formation. When the 1064 nm laser beam was focused into a H_2O or D_2O solution of PVME, we observed the formation of a single PVME microparticle at the focal point. However, obvious differences in the morphologies of the microparticles were detected between the H_2O and D_2O samples; these were the size, shape, and formation period of the microparticle. The origin of the behavior can be explained in terms of the optical absorbance of the solvent at the laser wavelength (1064 nm) as described below.

Figure 1a shows a series of optical micrographs of particles formed in H_2O as a function of laser power (P_{eff}). The threshold of P_{eff} to create a PVME microparticle was 40–50 mW. Irrespective of the laser power at $P_{eff} > 40$ mW, a single PVME microparticle appeared immediately after laser irradiation (<0.1 s), and reached an equilibrium state within 1.0 min. The single PVME microparticles produced were laser-trapped simultaneously at the focal spot of the incident 1064 nm laser beam. The optical micrographs in Fig. 1 were taken at equilibrium. As seen in the figure, the size and morphology of the microparticles was apparently sensitive to P_{eff}. The equilibrium size (diameter) of the particle increased with an increase in P_{eff}, as shown in Fig. 1b. Furthermore, the morphology of the PVME particle was also dependent on P_{eff}. At around the threshold value of P_{eff}, a single PVME microparticle with a diameter of less than 2 μm was observed at the focal spot of the laser beam, and the particle had a spherical morphology. For P_{eff} of up to ≈100 mW, the particles showed double-layered structures with the cores being surrounded by

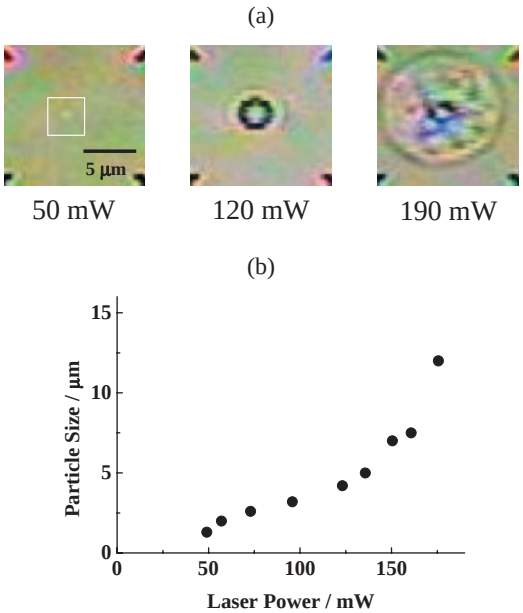

Fig. 1. (a) Optical micrographs of laser-induced PVME microparticles in H_2O. The laser power (P_{eff}) is given in the figure. Scale: bar = 5 μm. (b) Equilibrium size of the particle as a function of laser power.

thin shell structures. Such double-layered structures were more apparent at $P_{eff} = 190$ mW, Fig. 1a. In the PVME microparticle formed at $P_{eff} = 190$ mW, convection of the solution was clearly observed in the region between the core and the shell in the structure. The PVME microparticle produced by 1064 nm laser irradiation disappeared immediately after switching off the laser beam.

The laser-induced PVME microparticle formation in H_2O described above can be interpreted as occurring within the framework of the photothermal mechanism, since H_2O absorbs 1064 nm laser light through the overtone band of the O–H vibrational mode, as mentioned previously. In H_2O, laser-induced phase separation (microparticle formation) of a PVME solution is caused by local heating of the solution via the photothermal mechanism. The dependence on P_{eff} of the particle size shown in figure can be ascribed to heat diffusion around the focal point in the solution. Also, the double-layered structure can be explained on the basis of heat diffusion. The boundary between the solvent and the PVME particle growing by the heat diffusion should be clearly observed due to the difference in their refractive index.

We also examined laser-induced phase separation in a D_2O solution of PVME. Since D_2O (and PVME) is transparent at 1064 nm, the photothermal effect mentioned above is negligible.[11,22,23,34,36] Optical micrographs of the solution are shown in Fig. 2, and apparently, the phenomena observed in D_2O differ from those in H_2O. Immediately after laser irradiation ($P_{eff} = 80$–250 mW), no PVME particle was seen to form under a microscope. Upon prolonged 1064 nm laser irradiation (1–2 min.), however, a single PVME particle was produced, and several minutes after switching on the laser, the particle reached an equilibrium state as shown in the optical micrographs displayed in Fig. 2. As seen in the figure, the threshold value of P_{eff} for PVME microparticle formation (80 mW) was

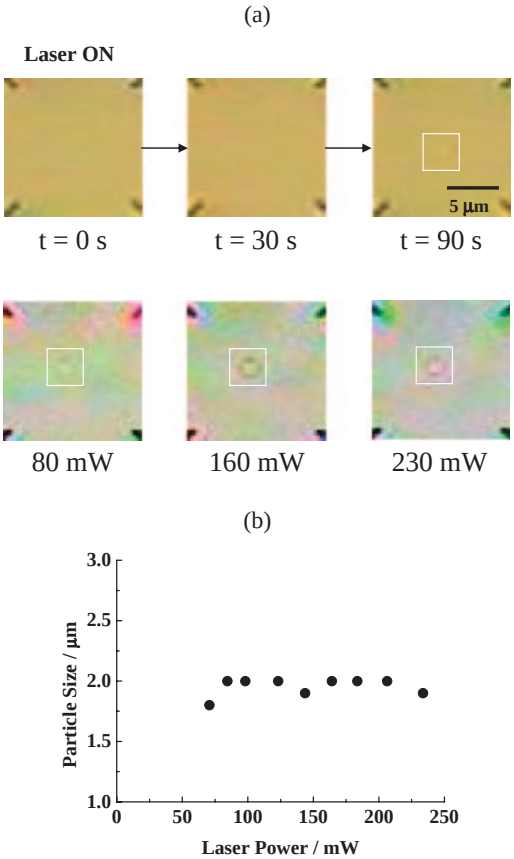

Fig. 2. (a) Optical micrographs of laser-induced PVME microparticles in D_2O. Upper panel: Temporal evolution of a microparticle formed at 80 mW. Lower panel: particles at equilibrium. The laser power (P_{eff}) is given in the figure. Scale: bar = 5 μm. (b) Equilibrium size of the particle as a function of laser power.

twice as large as that in H_2O ($P_{eff} = 40$ mW), and the diameter of the microparticles in equilibrium was constant at a value of 2 μm, irrespective of P_{eff}. This is in marked contrast to the result in H_2O, where the particle size increased with an increase in P_{eff}. The morphology of the microparticle was very ambiguous, and no convection was observed in the solution around the microparticle. Furthermore, the time necessary for particle dissociation after switching off the laser beam was several tens of seconds. As previously described, since photothermal effects are completely negligible in D_2O, the formation/dissociation process and the morphology of the microparticles are essentially different from those observed in H_2O. The origin of particle formation in D_2O is ascribed to molecular assembling of PMVE polymer chains by photon pressure of the focused laser beam. The structure of the PVME particle formed by photon pressure should be tighter than that formed in H_2O due to attractive interactions among polymer chains, resulting in the much longer disappearance time observed in previous works on PNIPA.[11,34]

Raman Spectra of the PVME Coil, Globule, and Microparticles. Although laser-induced microparticle formation was observed both in H_2O and D_2O, the characteristics of the two systems are very different, as described above and shown in Figs. 1 and 2. In order to examine the structure of

the PVME microparticles in H_2O and D_2O, therefore, we conducted Raman microspectroscopy. The molecular structure of thermo-responsive polymers upon phase transition, including PNIPA and PVME, can be well analyzed by Raman spectroscopy, since Raman spectra are highly sensitive to structural differences between hydrated-coiled and dehydrated-globular states.

Figure 3 displays the Raman spectrum of the PVME microparticle formed in D_2O ($P_{eff} = 190$ mW), together with those of PVME in the coiled and the globular states in D_2O as references. The reference spectra for the coiled and globular states were measured at room temperature and 310 K, respectively. For all the samples, various Raman bands were observed over a wide wavenumber region, and the assignment of the bands, based on the literature, are summarized in Table 1.[28–31] It is worth noting here that, since the Raman scattering intensity of PVME is very weak, particularly in the region of <2000 cm^{-1}, the spectrum in a dilute solution has not been reported, so far. Therefore, this is, to the best of our knowledge, the first report of the Raman spectra of PVME in a dilute solution.

First, we discuss the spectral differences between the coiled and globular PVME. As seen from Fig. 3 and Table 1, the Raman spectra of the coiled and globular states were similar in the wavenumber region below 1500 cm^{-1}. By contrast, significant differences in the spectra were observed between the two states in the wavenumber region of 2500–3000 cm^{-1}, as the expanded spectra shown in Fig. 4. Figure 4a shows the Raman bands of the O–D stretching mode of D_2O for the three

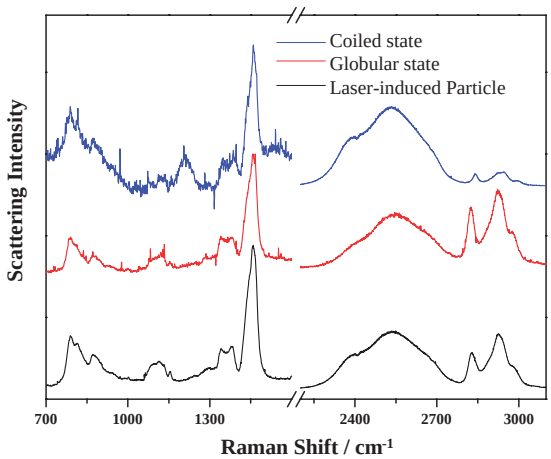

Fig. 3. Raman spectra of coiled state (blue line), globular state (red line), and a laser-induced microparticle formed at $P_{eff} = 190$ mW (black line) in D_2O.

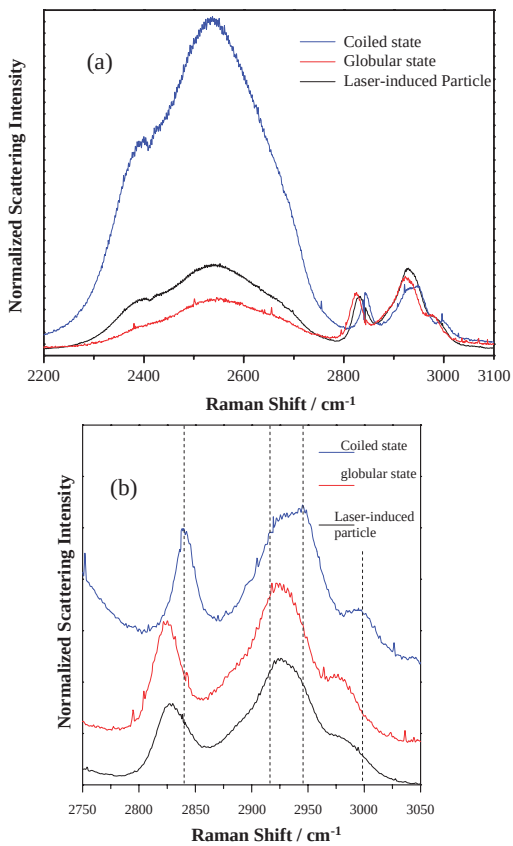

Fig. 4. Expanded Raman spectra of coiled state (blue line), globular state (red line), and a laser-induced microparticle formed at $P_{eff} = 190$ mW (black line) in D_2O. Wavenumber region: (a) 2200–3100 cm^{-1}. (b) 2750–3050 cm^{-1}.

Table 1. Raman Frequencies and Assignments of the Individual Bands Observed for the Laser-Induced Particles and the Coiled and Globular States in D_2O Solution[a)]

Wavenumber/cm^{-1}			
Laser-induced Particle	Coiled state	Globular state	Assignments
790, 813, 870	790, 815, 813	790, 813, 870	C–C skeletal vibration
1070	1070	1070	C–O stretching
1113	1112	1112	C–O stretching + C–H rocking
	1210		O–D bending of D_2O
1341, 1383	1347, 1386	1340, 1382	H–C–H bending
1459	1459	1458	H–C–H bending
2540	2530	2545	O–D stretching of D_2O
2825	2840	2825	Symmetric C–H stretching of CH_3
2925	2925	2925	Antisymmetric CH stretching of CH_2, dehydrated
	2945		Antisymmetric CH stretching of CH_2, hydrated
2975	2995	2975	Antisymmetric CH stretching of CH_3

a) The assignments were done on the basis of Refs. 28–31.

systems where the intensities are normalized to that at 2830 cm^{-1} (symmetrical C–H stretching mode of CH_3). The Raman signal intensity of the O–D stretching mode in the region of 2300–2700 cm^{-1} decreased appreciably upon thermal phase transition from the coiled state to the globular state, since phase transition is accompanied by dehydration of the polymer chain. The spectral differences between the samples were more pronounced in the region of 2800–3050 cm^{-1}, as shown in Fig. 4b. The coiled PVME showed the CH_3 symmetrical and antisymmetrical stretching bands at 2840 and 2995 cm^{-1}, respectively, whereas the bands were shifted toward lower wavenumbers (2825 and 2975 cm^{-1}, respectively) for globular PVME. The methylene C–H stretching vibrational band of coiled PVME at around 2940 cm^{-1} was split into two peaks at 2925 and 2945 cm^{-1}, and the latter peak was more intense compared with the former. For globular PVME, the relative intensity of the two peaks was reversed, and the peak at 2945 cm^{-1} was barely discernible.

Such spectral behavior can be interpreted as follows. It has been shown by Raman spectroscopy of a thermo-responsive polymer that the C–H stretching band of the polymer exhibits a slight low-frequency shift by dehydration of the C–H group.[24–33] The change in the relative intensity of the peaks of the antisymmetric CH stretching of $–CH_2–$ (2925 and 2045 cm^{-1}) upon phase transition from the coiled state to globular state is ascribed to dehydration of the methylene chain of the polymer in the globular state. Therefore, the changes in the relative peak intensities are evidence of the phase transition. Indeed, analogous spectral changes have been observed for an aqueous PVME solution by Maeda et al.,[28–31] as well as for other thermo-responsive polymers, such as PNIPA and related polymers.[24–27] Such behavior has also been observed for PVME in H_2O and for the PNIPA system.[34]

Here, we discuss the structure of the PVME particles produced by 1064 nm laser irradiation on the basis of the present experimental results and the above discussions. It is safe to say that the PVME microparticle formation in H_2O, shown in Fig. 1, is ascribable to photothermal effects. In practice, the Raman spectrum of the PVME microparticle produced by laser irradiation was in good agreement with that of globular PVME in H_2O, as shown in Fig. 5. The spectral assignments are the same as in Fig. 4. By contrast, as described previously, the photothermal effects are negligible in D_2O, since it is transparent at 1064 nm. Therefore, the structure of PVME microparticles produced by non-thermal phase transition is worth discussing here. As clearly seen in Figs. 3 and 4, the Raman spectra of the laser-induced particles were almost identical to that of globular PVME, but not explained by that of the coiled state. The expanded spectra in Fig. 4a demonstrate that the signal intensity of the O–D stretching mode observed for the laser-induced microparticle is much weaker than that of coiled PVME, and slightly stronger than that of globular PVME. This suggests that D_2O molecules hydrating the PVME polymer chains before laser irradiation are excluded upon particle formation at the focal point of the laser beam, and the content of D_2O molecules in the particle is rather close to that in globular PVME.

Furthermore, in the spectra of the methyl and methylene vibrational modes in the region of 2800–3000 cm^{-1} (Fig. 4b),

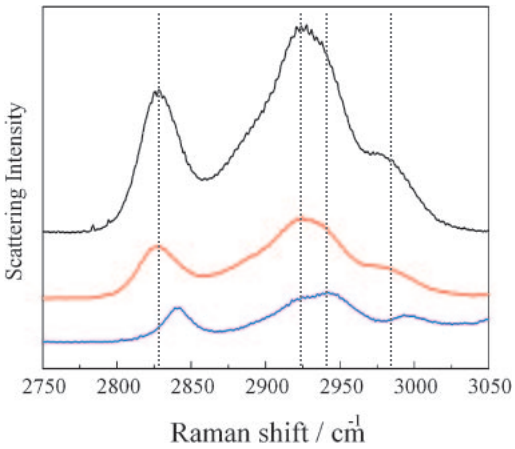

Fig. 5. Expanded Raman spectra of coiled state (blue line), globular state (red line), and a laser-induced microparticle formed at $P_{eff} = 120$ mW (black line) in H_2O.

the slight low frequency shift of the $–CH_3$ symmetric/antisymmetric stretching bands and the inversion of the relative ratio of the antisymmetric CH stretching of $–CH_2–$ (2925 and 2045 cm^{-1}) stretching bands observed for the globular state were reproduced in the spectrum of the laser-induced microparticle. This spectral behavior has been commonly observed for the microparticles irrespective of laser power. On the basis of the present observations, we conclude that the structure of laser-induced PVME microparticles is globular. Microparticle formation (phase separation) following the phase transition from a coil to a globule is triggered by laser irradiation.

Mechanism of Laser-Induced Particle Formation in D_2O. The driving force behind PVME molecular assembly in D_2O is clearly not due to the photothermal effects, but to the photon pressure produced by the laser beam, of which the origin is the dipole gradient force. As reported by Ashkin, the free energy of a system becomes lower when more polarizable molecules replace D_2O molecules at the focal point of a laser beam.[13,14] In the present case, coiled PMVE molecules dissolved in water can be regarded as Rayleigh particles, since the hydrodynamic radius of the coil ($r = 45$ nm on average) is much smaller than the wavelength of the incident laser beam (1064 nm). In this instance, the photon pressure exerted on a Rayleigh particle can be expressed on the basis of the Lorentz force,[12]

$$F = \frac{1}{2}\alpha\nabla\boldsymbol{E}^2 + \alpha\frac{\partial}{\partial t}(\boldsymbol{E}\times\boldsymbol{B}), \tag{1}$$

where $\boldsymbol{E}$ and $\boldsymbol{B}$ are the electric field strength and incident magnetic flux density, respectively. α is the polarizability of the particle (coiled PVME), which is given as:

$$\alpha = 4\pi\varepsilon_2 r^3\frac{(n_1/n_2)^2 - 1}{(n_1/n_2)^2 + 2}, \tag{2}$$

where ε_2 is the dielectric constant of D_2O, and n_1 and n_2 are the refractive indices of the particle and the surrounding medium (D_2O), respectively. In Eq. 1, the first term corresponds to the gradient force, and the second term acts on the particle as a scattering force due to the change in the Poynting vector of incident light. For $n_1 > n_2$, the gradient force is directed to a

high intensity electric field region, i.e., the focal point. In the present case, using a focused near-infrared Gaussian laser beam, the gradient force is much stronger than the scattering force. Accordingly, the particle is attracted and trapped at the focal point of the laser beam by the radiation force. In this case, the potential energy (U) for optical trapping is expressed as follows:

$$U = -\alpha \boldsymbol{E}^2/2. \quad (3)$$

Under the present conditions of $P_{\text{eff}} > 80\,\text{mW}$, n_1 (refractive index of PVME) = 1.462, and with the diameter of the laser spot being $\approx\lambda$ (=1064 nm), r should be >25 nm to satisfy the trapping condition, $U > k_{\text{B}}T$, where k_{B} and T are the Boltzmann constant and absolute temperature, respectively. Therefore, PVME coils ($r = 45\,\text{nm}$) can be trapped at the focal point of the laser beam and assemble together, overcoming the Brownian motion of the polymer coils. Thus, single PVME microparticles are produced through the photon pressure.

During molecular assembly of the polymer coils, coiled PVME molecules become closer to each other due to photon pressure, as described above. This results in an increase in the hydrophobic interactions between PVME coils as opposed to the hydrophilic interactions between the coils and D_2O, leading to a phase transition from the coiled state to the globular state. In the case of thermally induced (thermo-responsive) processes in H_2O, the phase transition is followed by phase separation. In contrast, as a tentative explanation, we think that the phase transition follows phase separation (microparticle formation) in D_2O. The mechanism proposed holds also for laser-induced PNIPA microparticle formation in D_2O, as reported previously.[34]

Finally, we briefly compare behaviors of particle formation in D_2O between PVME and PNIPA.[11,34] The threshold P_{eff} values of the particle formation for the each system were similar (<100 mW), as determined from microscope observations. However, the PVME particle has very ambiguous morphology as compared to the PNIPA system. Furthermore, the growth rate of the particle in the PVME system was somewhat slower than that in the PNIPA system. Both the refractive index and molecular weight of PVME used in the present study (n = 1.462 and $M_{\text{w}} = 9 \times 10^4$) were lower than those of PNIPA used in the previous study ($n = 1.508$ and $M_{\text{w}} = 5.2 \times 10^5$).[34] These lower n and M_{w} values make the interaction energy U small. This is the origin of the observed difference between PVME and PNNIPA systems.

The authors are grateful to Prof. H. Misawa (Hokkaido University), Dr. S. Ito (Osaka University), and Dr. O. Urakawa (Osaka University) for their helpful discussions. The authors also thank Prof. M. Shimomura (Hokkaido University) for the use of the apparatus of dynamic light scattering. YT acknowledges Yamada Science Foundation for financial support. This work was supported in part by a Grant-in-Aid from the Ministry of Education, Culture, Sport, Science and Technology of Japan (No. 18550002).

References

1 M. Heskins, J. E. Guillet, *J. Macromol. Sci., Chem. A* **1968**, *2*, 1441.
2 O. B. Ptisyn, A. K. Kron, Y. Y. Eizner, *J. Polym. Sci., Part C* **1968**, *16*, 3509.
3 S. Fujishige, K. Kubota, I. Ando, *J. Phys. Chem.* **1989**, *93*, 3311.
4 H. Hu, X.-D. Fan, *J. Funct. Polym.* **2000**, *13*, 451.
5 R. A. Horne, J. P. Almeida, F. A. Day, N.-T. Yu, *J. Colloid Interface Sci.* **1971**, *35*, 77.
6 Y. Hirokawa, T. Tanaka, *J. Chem. Phys.* **1984**, *81*, 6379.
7 N. A. Peppas, *Hydrogels in Medicine and Pharmacy*, CRC Press, Boca Raton, **1987**.
8 V. O. Aseyev, H. Tenhu, F. M. Winnik, *Advances in Polymer Science*, **2006**, Vol. 196, p. 1.
9 M. Ishikawa, H. Misawa, N. Kitamura, H. Masuhara, *Chem. Lett.* **1993**, 481.
10 M. Ishikawa, H. Misawa, N. Kitamura, R. Fujisawa, H. Masuhara, *Bull. Chem. Soc. Jpn.* **1996**, *69*, 59.
11 J. Hofkens, J. Hotta, K. Sasaki, H. Masuhara, K. Iwai, *Langmuir* **1997**, *13*, 414.
12 Y. R. Shen, *The Principles of Nonlinear Optics*, Wiley-Interscience, New York, **1984**, pp. 366–378.
13 A. Ashkin, *Phys. Rev. Lett.* **1970**, *24*, 156.
14 A. Ashkin, *Proc. Natl. Acad. Sci. U.S.A.* **1997**, *94*, 4853.
15 N. Kitamura, F. Kitagawa, *J. Photochem. Photobiol., C* **2003**, *4*, 227.
16 H. Misawa, M. Koshioka, K. Sasaki, N. Kitamura, H. Masuhara, *J. Appl. Phys.* **1991**, *70*, 3829.
17 M. P. Houlne, C. M. Sjostrom, R. H. Uibel, R. J. A. Kleimeyer, J. M. Harris, *Anal. Chem.* **2002**, *74*, 4311.
18 K. Ajito, *Appl. Spectrosc.* **1998**, *52*, 339.
19 C. Bustamante, Z. Bryant, S. B. Smith, *Nature* **2003**, *421*, 423.
20 D. J. Odde, M. J. Renn, *Biotechnol. Bioeng.* **2000**, *67*, 312.
21 S. Masuo, H. Yoshikawa, T. Asahi, H. Masuhara, T. Sato, D.-L. Jiang, T. Aida, *J. Phys. Chem. B* **2002**, *106*, 905.
22 S. Juodkazis, N. Mukai, R. Wakai, A. Yamaguchi, S. Matsuo, H. Misawa, *Nature* **2000**, *408*, 178.
23 J. Hofkens, J. Hotta, K. Sasaki, H. Masuhara, T. Taniguchi, T. Miyashita, *J. Am. Chem. Soc.* **1997**, *119*, 2741.
24 Y. Maeda, T. Higuchi, I. Ikeda, *Langmuir* **2000**, *16*, 7503.
25 Y. Maeda, T. Nakamura, I. Ikeda, *Macromolecules* **2001**, *34*, 1391.
26 Y. Maeda, T. Nakamura, I. Ikeda, *Macromolecules* **2001**, *34*, 8246.
27 Y. Maeda, H. Yamamoto, I. Ikeda, *Macromolecules* **2003**, *36*, 5055.
28 Y. Maeda, *Langmuir* **2001**, *17*, 1737.
29 Y. Maeda, H. Mochiduki, H. Yamamoto, Y. Nishimura, I. Ikeda, *Langmuir* **2003**, *19*, 10357.
30 Y. Maeda, H. Yamamoto, I. Ikeda, *Langmuir* **2004**, *20*, 7339.
31 Y. Maeda, H. Yamamoto, I. Ikeda, *Macromol. Rapid Commun.* **2004**, *25*, 720.
32 Y. Katsumoto, T. Tanaka, H. Sato, Y. Ozaki, *J. Phys. Chem. A* **2002**, *106*, 3429.
33 Y. Katsumoto, T. Tanaka, Y. Ozaki, *J. Phys. Chem. B* **2005**, *109*, 20690.
34 Y. Tsuboi, M. Nishino, T. Sasaki, N. Kitamura, *J. Phys. Chem. B* **2005**, *109*, 7033.
35 H. Yan, M. Nishino, Y. Tsuboi, K. Tsujii, *Langmuir* **2005**, *21*, 7076.
36 S. Ito, T. Sugiyama, N. Toitani, G. Katayama, H. Miyasaka, *J. Phys. Chem. B* **2007**, *111*, 2365.